Extraction of Aluminum from Astronaut Waste Food Packaging for In-Space Manufacturing

Ray P. Pitts[1], Marisa D. Kelley[2], and Jackson L. Smith[3]
National Aeronautics and Space Administration, Kennedy Space Center, FL, 32899, USA

The sustainable human presence beyond low earth orbit is contingent on the effective use of local resources, what has since been termed in-situ resource utilization (ISRU). Metal extraction from lunar and Martian regolith has become a significant area of interest for the ISRU community, enabling in-situ production of metallic equipment, spares, and construction materials for various mission scenarios. However, the extraction of metals from the astronaut waste stream has yet to be thoroughly investigated. A thermochemical Trash-to-Gas (TtG) process was utilized to isolate pure aluminum (Al 1235) from multilayer astronaut waste food packaging, one of the most abundant crew waste items expected for future exploration missions. The extracted aluminum was post-processed to enable compatibility with the bound metal deposition (BMD) additive manufacturing process. The aluminum was cleaned, converted into a powder, and incorporated into an aluminum paste mixture to enable effective extrusion of the material. The particle size distribution, morphology, oxygen content, and elemental composition of the extracted aluminum powder is reported. The results described herein demonstrate an end-to-end waste metallic reuse process which may garner considerable metal recovery and reutilization that would otherwise be disposed of on future exploration missions.

Nomenclature

Al	=	aluminum
Ar	=	argon
BMD	=	bound metal deposition
COTS	=	commercial off the shelf
ECLSS	=	environmental control and life support systems
HDPE	=	high density polyethylene
ISM	=	in-space manufacturing
ISRU	=	in-situ resource utilization
kg	=	kilogram
KSC	=	Kennedy Space Center
LDPE	=	low density polyethylene
mg	=	milligram
MSFC	=	Marshall Spaceflight Center
nm	=	nanometer
O_2	=	oxygen
OSCAR	=	Orbital Syngas/Commodity Augmentation Reactor
PET	=	polyethylene terephthalate
RSD	=	relative standard deviation
SEM	=	scanning electron microscopy
TtG	=	Trash-to-Gas
XPS	=	X-ray photoelectron spectroscopy
YSZ	=	Yttria-stabilized zirconia

[1] Research Engineer, Exploration Systems and Development Office, NASA KSC
[2] Pathways Intern, Exploration Systems and Development Office, NASA KSC
[3] Pathways Intern, Exploration Systems and Development Office, NASA KSC

I. Introduction

In-situ resource utililzation (ISRU) is considered a vital element in establishing the sustained human presence on other planetary bodies. Accordingly, NASA has made long-term investments toward the development of ISRU technologies, with a particular focus on regolith-based resource extraction, processing, and construction, as well as Martian atmosphere resource extraction and processing. However, the resource-potential of waste materials brought from Earth is now being considered. Waste materials can be a source of various resources, including but not limited to metals, polymers, water, carbon, propellant, and energy (e.g., trash-to-energy processing). Due to the variety of resources within the waste stream, a multitude of functions are possible, contingent on the production rate of each respective waste resource[1].

One prospective function for waste material is the production of in-situ derived feedstock for in-space manufacturing and construction. Polymers (e.g., polyethylene, polyester, polypropylene) and metals (e.g., aluminum, titanium) are found in the waste stream and are feedstocks that are compatible with various in-space manufacturing methods. To better highlight the expected waste material composition for future human exploration missions, a waste model was developed detailing both the elemental and material composition of crew consumable waste[2]. From this analysis, aluminized astronaut food packaging (Glenroy Inc. EFO 289-001) was identified as a waste item with one of the highest generation rates. From the elemental analysis performed on this multilayer food packaging, it was found to contain approximately 29.5 wt% of aluminum alloy 1235. At the expected production rate of food packaging waste for a crew of four, this would amount to nearly 75 kg/year of pure aluminum waste[2,3]. This commodity rate scales with both mission duration and crew size as longer and larger exploration missions are realized. Furthermore, aluminum waste is not limited to the food packaging material alone; it is a common material in spent equipment, broken parts, structures, and other waste hardware items that may be found locally. Thus, the aluminum waste generation rate is non-trivial, providing a source of in-situ aluminum feedstock while reducing the amount of waste material that is stored long-term on the surface of other planetary bodies.

The extraction of aluminum from multilayer packaging material synergizes particularly well with NASA's development of Trash-to-Gas (TtG): the use of a thermochemical process to convert waste items into more useful gaseous, liquid, or solid products. Depending on the desired end products, various thermochemical processes can be utilized. NASA has performed trade studies comparing the performance of several thermochemical processes including combustion, incineration, steam reforming, torrefaction, ozonation, pyrolysis, and plasma pyrolysis [4–6].The results of these trade studies identified combustion, steam reforming, and pyrolysis as high-performing candidates for various space applications including Environmental Control and Life Support Systems (ECLSS) commodity production, trash mass & volume reduction, and resistojet propellant production. Of the three high-performing TtG processes, only combustion has been demonstrated in microgravity as part of a suborbital flight campaign of the Orbital Syngas/Commodity Augmentation Reactor (OSCAR) [7,8]. Reactor temperature profiles, both in microgravity and in Earth gravity, observed a mean temperature within the reactor hearth zone of approximately 400° C[7]. This average combustion temperature is effective in gasifying the vast majority of materials present in the astronaut waste stream including textiles (e.g., clothing, cotton towels), food waste, polymers, and metabolic waste. However, the astronaut food packaging waste contains an inner sheet of pure aluminum foil, layered with various polymers including polyester, low density polyethylene (LDPE), and SURLYN™. Due to the combustion process, all of the polymer layers are effectively converted into gas, leaving the aluminum foil, with a melting point of approximately 660° C, as the primary solid product post-reaction. Thus, the TtG process effectively isolates the aluminum layer within astronaut food packaging which would otherwise be disposed of.

Aluminum recovery from in-situ resources is of high-value to NASA's goal of sustaining the human presence in space. Aluminum is of particular high utility due to its potential in producing large-scale surface structures as well as small-scale parts, tools, and equipment. Aluminum has become an integral material in the portfolio of the In-Space Manufacturing (ISM) research group at NASA Marshall Spaceflight Center (MSFC). ISM aims at identifying, designing, and implementing on-demand, sustainable manufacturing solutions for fabrication, maintenance, and repair during exploration missions[9]. One additive manufacturing technique that has been developed for space applications is the bound metal deposition (BMD) process. BMD is an additive manufacturing process that extrudes metal via powder-filled thermoplastic media followed by inert gas sintering. This process is compatible with aluminum alloys and could be used to produce additive manufactured parts extracted from various in-situ resources including waste materials and regolith. Thus, the primary solid by-product of the TtG process, pure aluminum, could be repurposed as additive manufacturing feedstock via BMD, increasing the technology's resource recovery potential. This technologic synergy between TtG and ISM yielded the first demonstration of an end-to-end recycling process of astronaut multilayer food packaging. The mixed polymeric layers were combusted via TtG into mainly water and carbon

dioxide; water was condensed and collected for life support or fuel considerations; carbon dioxide was collected and could be used to produce methane (i.e., fuel) via the Sabatier process; and now the solid products (aluminum) can be collected and assessed as a candidate feedstock for in-space additive manufacturing. This form of waste management collaboration and coordination is a necessary step in providing a sustainable waste management architecture for the Artemis generation and beyond. The results, lessons learned, and next steps of this end-to-end process are discussed.

II. Methods

A. Trash-to-Gas Methods

The aluminum extraction and preparation processes used for this study are shown in Figure 1. This consisted of TtG processing of aluminum-rich astronaut food packaging, followed by cleaning and preparation of the aluminum material for BMD additive manufacturing. Material analyses of the aluminum product were performed at varying stages of refinement. To use the extracted material as BMD feedstock, the aluminum from TtG needs to be cleaned and the aluminum product converted into a powder. After removal from the TtG reactor, the extracted aluminum sheets were initially cleaned with an alkaline wash (Alconox®) to remove any remaining soot generated by the polymer layers of the food packaging. The cleaned sheets were then powderized to 63 micrometers (µm) via high-energy ball milling. Once powderized to the correct particle size, the material was then shipped to the University of Louisville (UofL) from NASA Kennedy Space Canter (KSC) for additive manufacturing trials.

Several analytical methods were needed to better understand the material properties of the final aluminum product. Analytical methods were identified to best answer the following questions:

1. How does the thermochemical Trash-to-Gas process affect oxide layer thickness of the aluminum?
2. What is the ash composition on the surface of the aluminum material post-Trash-to-Gas, prior to cleaning?
3. What is the oxygen content of the final aluminum powder?
4. What is the particle size distribution of the final aluminum powder?

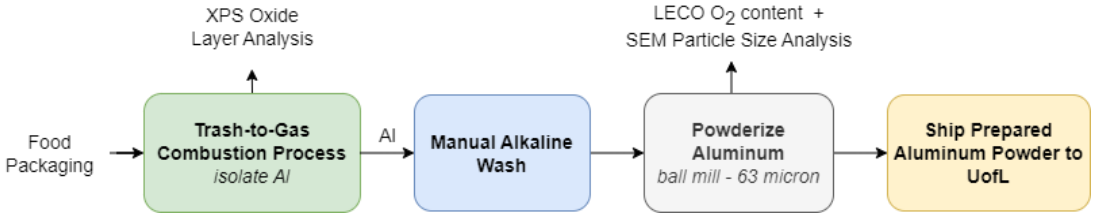

Figure 1. Aluminum Extraction Process Diagram

1. Trash-to-Gas Processing

Prior to performing large-batch TtG tests to produce the aluminum products for additive manufacturing trials, an initial comparison of aluminum oxide formation between combustion and pyrolysis TtG processes was performed to determine which method would be preferable for this application. Combustion, with the presence of oxygen during the reaction, has the potential of generating a thicker oxide layer on the surface of the pure aluminum. Increased oxides act as impurities which can lead to defects like pores and cracks during additive manufacturing [10]. Pyrolysis, on the other hand, thermally degrades the food packaging material in the presence of an inert environment. It was hypothesized that the increased oxygen concentration present in the combustion environment would lead to increased aluminum oxidation when burning the food packaging material, as compared to the oxygen-deficient environment of the pyrolysis process.

A commercial off the shelf (COTS) tube furnace was used for this study, rather than the OSCAR system, due to the limited throughput capacity (<20 grams) of the OSCAR suborbital flight system. Up to 85 grams of astronaut food packaging was manually placed into a Thermo Scientific Lindberg Blue M Tube Furnace containing a built-in three zone temperature control and upstream flow control to enable air combustion (21% O_2 environment) and pyrolysis (100% Ar environment). Both processes used a maximum final temperature setpoint of 600 °C. Pyrolysis mode utilized a heat ramp rate of 75 °C/min up to 250 °C, followed by 20 °C/min until a maximum temperature of 600°C was reached. Combustion used the 75 °C/min ramp rate continuously until the 600 °C temperature was reached. Once

at steady state temperature, both processes were maintained until full conversion of the food packaging material was confirmed. Full conversion was defined as when negligible gas production was observed via downstream flowrate data measured by a Mesa Labs Defender 510 flow meter.

50 grams of aluminum powder was needed per additive manufacturing test sample. Due to the lengthy ball milling process, it was determined that the test samples were to be prepared in duplicate. Thus, 100g of aluminum powder was collected from the TtG process. Air combustion (21% O_2) was used with the same heat rate parameters as described above with the exception of the final temperature being set to 500°C. Several TtG runs were performed to amass the required 100g of aluminum. Post-test, the aluminum products, in the form of a sheet, were manually removed from the TtG reactor and the cleaning procedures ensued.

2. Aluminum Cleaning

After the Trash-to-Gas process, various post-processing steps were taken to prepare the aluminum material for use in additive manufacturing. Due to the 1" diameter restriction of the tube reactor, the 6x6" food packaging material had to be folded several times to fit inside the tube. This was done, rather than shredding the material, to enable more efficient cleaning of the aluminum surface post-test. However, the folded food packaging did not allow for sufficient mixing of the oxidizer with the innermost folded material during the combustion process, likely increasing the soot formation on the surface. It should be emphasized that future aluminum extraction experiments which utilize a larger reactor designed to be compatible with the size of the test material will likely reduce the soot formation on the aluminum surface. Nonetheless, any remaining soot residue was effectively removed via manual cleaning with an Alconox® and DI water solution. This was achieved by lightly brushing the soot-covered surface with a Q-tip rinsed with the Alconox® and DI water solution. The process of isolating the aluminum layer via Trash-to-Gas combustion processing, followed by soot removal using the Alconox® solution for a single food packaging unit can be seen in Figure 2.

Figure 2. Original food packaging material (left), uncleaned aluminum layer post-TtG process (middle), and Alconox®-cleaned aluminum sheet (right)

3. Aluminum Powder Production

After cleaning, the aluminum sheets were then converted into a powder via a two-step particle size reduction process. First, the sheets were ground into a coarse, 400-micron powder using a Bel-Art® Micro-mill Grinder in an inert, nitrogen environment. This was done to expedite the time needed for the second step of the powder process: high-energy ball milling. A US Stoneware® benchtop jar mill was used for this operation. 100 grams of the coarse aluminum powder were put into a size 0 U.S Stoneware® alumina jar. 3 mm and 5 mm Yttria-stabilized zirconia (YSZ) balls were then placed into the jar to fill approximately 60% of the combined jar volume. The ball mill was placed into an inert, nitrogen environment using a benchtop inflatable glove bag and the jar mill was rotated at 76 revolutions per minute. The ball milling process was performed until all particles were below a 63-µm threshold; 63-µm was the target particle size to prevent clogging of the BMD extruder nozzle. This was achieved by sieving the

powder with a 61-µm sieve sheet and a benchtop vibratory bed. It should be noted that the ball milling process took significantly longer than had been reported in analogous studies [11]. The team observed a production rate of at-size particles of 1 g/hour of ball milling. Future works aiming to powderize aluminum should utilize a cryogenic mill, if possible, to increase the brittleness of the aluminum, thereby improving grinding efficiency. An image of the ball-milled powder and YSZ balls within the ceramic jar can be seen in Figure 3. Once 100 grams of 63-µm powder was produced, the aluminum powder was then shipped to the University of Louisville for the additive manufacturing trials.

Figure 3. Ball-Milled Aluminum Inside Jar with YSZ Balls

4. Aluminum Oxide Quantitation

X-ray Photoelectron Spectroscopy (XPS) was utilized to quantify the oxide thickness on the aluminum sheets generated from TtG in combustion and pyrolysis modes. 1x1 cm samples of the aluminum sheets were cleaned with Alconox® to remove any remaining soot and then analyzed on the XPS instrument. Depth profile measurements were performed to quantify the resultant aluminum oxide layer. The XPS instrument was configured with the following parameters: 1000 eV ion beam, 10 second scan time, 25 etch layers. The Thermo Fisher Scientific Avantage Data System software was used to process the XPS data. This software comes with a built-in single overlayer function which automatically determines oxide thicknesses for layers less than 10 nanometers (nm). For layers of oxide greater than 10 nm, the data were exported into a comma-separated values (csv) file, the slope of the oxide depth profile determined, and the oxide thickness calculated as the point where the elemental aluminum becomes present in the etching process. The combustion and pyrolysis samples were compared to raw aluminum foil (alloy 1235) as a control. Triplicate point data sets were performed for all samples.

To quantify the total oxygen content within the aluminum once converted into a powder, an oxygen content analysis was performed at the NASA KSC Cleaning, Refurbishment, and Chemical Analysis (CRCA) laboratory using a LECO model ONH 836 analyzer. Five 10 mg samples were analyzed on the shipped TtG aluminum powders and averaged to determine the oxygen content.

5. Particle Size Distribution & Morphology

Scanning Electron Microscope (SEM) was used to determine the particle size distribution of the final TtG powder and to assess the particle morphology. The samples for particle size analysis were prepared by mounting a thin, dispersed layer of powder onto carbon tape. This was done by spreading powder out on a plastic weigh boat so that there were visible gaps between powder particles. Then, a stub with carbon tape on it was stamped into the powder so it would adhere to the carbon tape. Two stubs with the ball milled TtG Al 1235 powder were prepared in this way. SEM images were taken of each sample at a magnification of 103x so that many powder particles were in each image. The location of the images on the sample were chosen based on where the powder was spread enough so that there were gaps between the powder particles.

The analysis of the images was done using the open-source software ImageJ. Within ImageJ is a built-in program for analyzing particles. The procedure for the analysis of the ball milled TtG Al 1235 powder was as follows: first, the scale bar in the SEM image was measured to set the pixel size to the µm scale for the image. After setting the correct scale, the image was cropped so only the powder was visible and the banner within the SEM image was removed. Following this, a slight gaussian blur was applied. The blur was on the order of 3 pixels and primarily smoothed the coloring of the particles. Without the filter, bright highlights on particles can be mistaken as separate entities by the software. The blur did not alter the size of the particles. After the blur filter, the contrast of the image was increased to make the powder more distinct against the background. The last step before analyzing the particles was to threshold the image so that all the particles would be white and the background black. Then, the 'analyze particles' function of the software was then used to automatically measure the circularity and size of every powder particle in the image. For the purpose of this analysis, any particles smaller than 10 pixels in area were not considered as powder. Additionally, the function was set to not consider any particle that had a circularity less than 0.2 to filter out likely fiber contaminants in the image. When the particle analysis function was applied, the software then produced an image with an overlay showing the outlines of each particle measured and a data table with the measurements. The 10^{th}, 50^{th}, and 90^{th} percentiles of powder diameter were then calculated.

To better visualize the morphology of the TtG Al 1235 powder that was shipped to UofL, separate SEM samples were prepared and imaged, as shown in Figure 5. For this application, carbon tape was placed on a SEM stub and a thicker film of the respective aluminum powder was coated onto the carbon tape by pressing the carbon tape into a sample of the powder; this was done to allow for an increased number of grains to be imaged per area. Note that this method does not allow for individual particles to be analyzed since particles are so closely packed that each grain boundary cannot be easily identified. Thus, these images were not used to assess particle size and were solely used to analyze the morphology of the particles. The SEM settings were set to 10.00 kV and a magnification of 130x to get a more detailed visualization of the powder particles.

6. TtG Solid Product Elemental Composition

Knowledge of the elemental composition of the extracted aluminum and accompanying ash residue, prior to cleaning, can help future recycling efforts determine whether rigorous cleaning methods are needed for certain use cases. To characterize the elemental composition of the aluminum sheet and residual ash content on the surface, a UNICUBE elemental analysis for carbon, nitrogen, and sulfur was performed. Carbon is the primary element of combustion ash and was thus the main focus of quantitation. 50 mg samples were prepared for this analysis for three different surface regions on the extracted aluminum sheet: Black Ash, Brown Ash, and No Ash. Referring to Figure 2, one can see regions of concentrated dark ash (i.e., Black Ash), slightly lighter concentrated regions (i.e., Brown Ash), and regions with little to no ash on the surface (i.e., No Ash). Note that the majority of the surface has little to no ash formation and that the ash formation was only produced on one side of the aluminum sheet. Each region was analyzed in triplicate and the average of the three carbon contents was reported as a conservative estimate on overall carbon content on the surface. Note that the elemental composition of the aluminum and ash material determined in this study is strictly for scenarios in which only food packaging is processed in a Trash-to-Gas reactor; if a more complex mixture of trash items are processed simultaneously, a much different ash composition would be produced.

III. Results & Discussion

A. Trash-to-Gas Results

1. Aluminum Oxide Quantitation

The initial comparison of oxide layer thicknesses between combustion, pyrolysis, and control samples via XPS analysis can be seen in Figure 4.

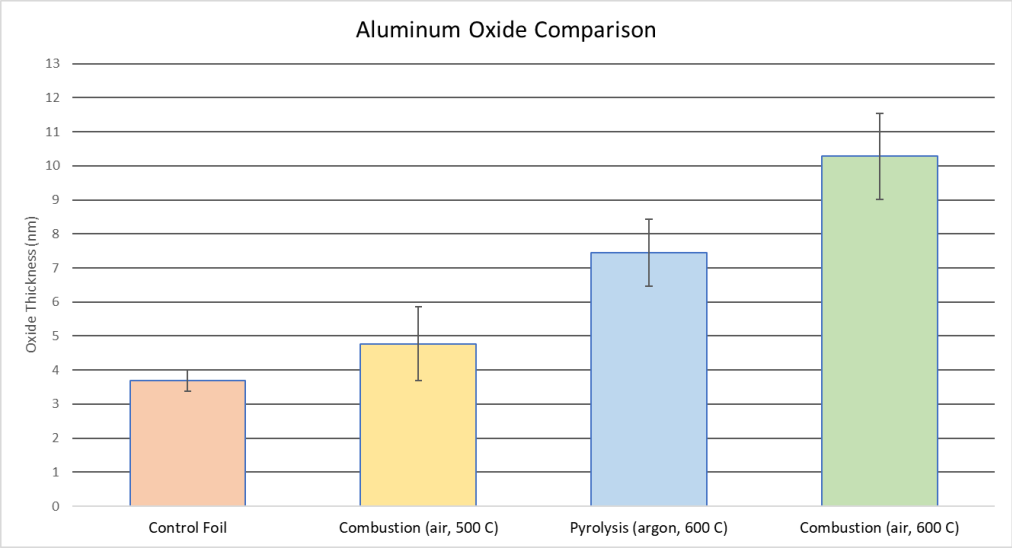

Figure 4. Aluminum Oxide Comparison of Control, Combustion, and Pyrolysis Aluminum Products

Pyrolysis and combustion samples at 600 °C exhibited thicker oxide layers than those observed in the control Al 1235 foil. This can be attributed to the increased temperatures that the aluminum was exposed to; at elevated temperatures approaching 600°C, aluminum oxide transitions into a γ-alumina phase which increases its crystallinity, enabling increased diffusion of oxygen into the material[12]. Combustion samples were also shown to have thicker oxide layers than pyrolysis samples at an equivalent test temperature, likely due to the increased oxygen availability during the thermal degradation process. However, when the final combustion temperature was decreased to 500 °C, the oxide formation was reduced to approximately 5 nm, within the bounds of the relative standard deviation (RSD) of the control sample triplicate. The 5 nm oxide thickness agrees with previously reported critical amorphous oxide thicknesses prior to γ-alumina phase change[12].

Although combustion was shown to have a slightly higher oxide thickness when compared to pyrolysis at equivalent steady state temperature, combustion was ultimately down selected for use in this study. This was determined due to the overall cleanliness of the aluminum product and the effectiveness of combustion in processing large batches of food packaging within the tube furnace apparatus. During pyrolysis runs, considerable wax and tar formation occured on the surface of the aluminum product which made it challenging to clean and prepare the samples for powder production and subsequent additive manufacturing. A single aluminum sheet (approximately 2 grams) would take upwards of one hour to clean the tar and wax residue; combustion aluminum sheets typically took 1-2 minutes to clean, in comparison. Furthermore, by lowering the combustion maximum temperature to 500 °C, the oxide layer decreased, nearing the typical oxide layer thickness observed on control aluminum foil samples. These findings gave the team sufficient rationale to utilize the combustion process as the aluminum extraction mode for this research.

Results of the LECO oxygen content analysis can be seen in Table 1.

Table 1. Oxygen Content of TtG Al 1235

Sample ID	Oxygen Content (%)	Relative Standard Deviation (%)
TtG Al 1235 Powder	3.53%	± 37.99%

It was observed that the TtG Al 1235 powder contained approximately 3.53% oxygen. This is considerably higher than what has been previously reported for atomized aluminum powders[13]. This material was intermittently ball

milled in an inert environment for upwards of 100 hours. The operating conditions during high energy ball milling, particularly the temperature profile, likely affected the oxide formation during the powder process as compared to more traditional atomization processes. The initial grinding process prior to ball milling could also have affected the temperature of the aluminum powder, thereby affecting oxidation rates. These samples also exhibited high relative standard deviations, in the range of ± 38%. The cause of such variability is not well understood as the samples were homogenized, consisting of cleaned Al 1235 powder.

2. Particle Size Distribution & Morphology

SEM images of the TtG Al 1235 powder for morphology assessments and particle size analysis are shown in Figure 5.

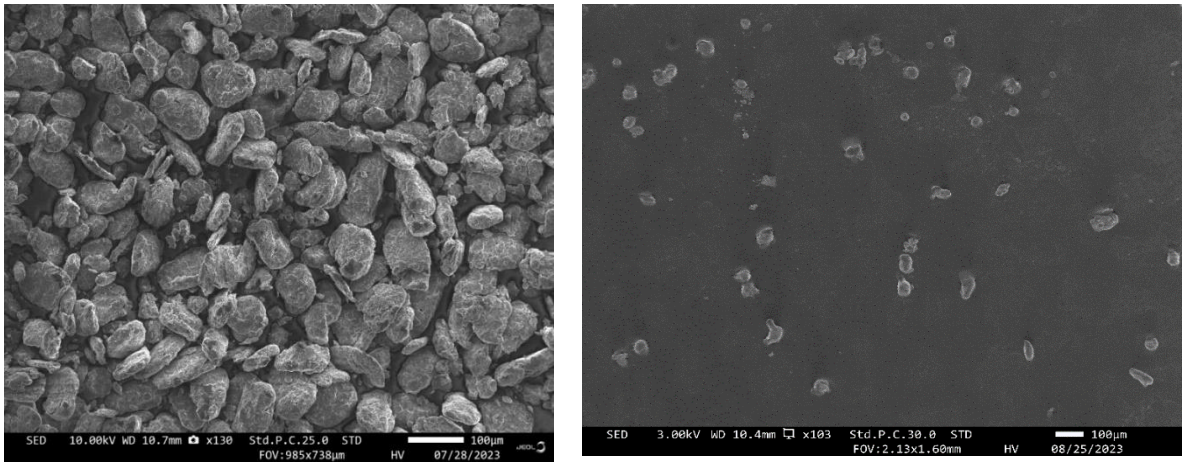

Figure 5. SEM Image of TtG Al 1235 Used for Morphology (left) and TtG Al Powder Used for Particle Size Analysis (right)

From these images, the 10th, 50th, and 90th percentiles of powder diameter were calculated. These results are shown in Table 2. The 90th percentile of particles for the TtG Al 1235 powder was determined to be 55.7 µm, slightly smaller than the threshold of 63 µm. This smaller particle size may be preferable as it allows for more densely packed parts within the extrusion and sintering processes of BMD. However, smaller particles lead to increased surface area exposure for aluminum oxidation, which may have contributed to the increased oxygen content observed.

Table 2. Powder Diameter Percentile for TtG Al 1235 Powder.

Diameter Percentile	TtG Al 1235 Diameter (µm)
10	4.9
50	14.5
90	55.7

As seen in the left image of Figure 5, the TtG Al 1235 powder appears flattened and oblong, comparable to previously reported aluminum powders via high energy ball milling with a high ratio of large to small ball sizes [14]. Note that both 3 mm and 5 mm YSZ balls were used for this study but the ratio of the two ball sizes was not determined. These irregular particle shapes may improve packing density during additive manufacturing as compared to spherical particles [15].

3. TtG Solid Product Elemental Composition

Carbon, nitrogen, and sulfur weight percentages for uncleaned, TtG Al 1235 sheets are shown in Table 3. Three samples of the TtG Al 1235 material were analyzed: Black Ash, Brown Ash, and No Ash, as can be seen in Figure 2. It was hypothesized that the darker colored ash materials were made up of increased soot layers and this was confirmed

with the carbon analysis shown in Table 3. As can be seen, carbon makes up approximately 22.76% of the surface covered in Black Ash, 7.22% of the Brown Ash, and only 1.75% of the No Ash samples. For a conservative estimate, it was assumed that each of these samples make up equal proportions of the aluminum product that would be extracted from the TtG reactor, yielding an average carbon content of approximately 10.6%. At the test conditions used for TtG combustion processing, carbon is likely the major ash constituent on the surface of the aluminum, although there are likely other trace elements present on the surface. Nonetheless, with this conservative estimate, the material that is directly extracted out of a Trash-to-Gas system would contain at least 89.4% aluminum/alumina that could be used for additive manufacturing, prior to cleaning. If this degree of purity is sufficient, simple and effective automated removal processes of aluminum from a TtG reactor could be realized.

Table 3. Carbon, Nitrogen, Sulfur Weight Percent of Aluminum Ash from TtG

Ash Type	C (%)	N (%)	S (%)
Black Ash	22.76	0.18	0
Brown Ash	7.22	0.1	0
No Ash	1.75	0	0
Avg	**10.58**	**0.09**	**0.00**
St Dev.	10.89	0.09	0.00

IV. Conclusion

The extraction of waste aluminum products originally contained within composite astronaut food packaging and subsequent preparation for BMD additive manufacturing was performed. Pure aluminum was isolated from various polymeric layers via Trash-to-Gas combustion processing at 500 °C. The aluminum was then cleaned and converted into a powder via high energy ball milling to generate a 90^{th} percentile particle size of approximately 55.7 µm to ensure compatibility with BMD additive manufacturing. The oxygen content of the extracted aluminum was determined to be 3.53 ± 1.34%. At the time of this writing, the BMD additive manufacturing trials of the TtG aluminum powder are still in progress. A future publication will focus on the results and lessons learned from the BMD production of aluminum parts. The results described herein demonstrate the first metallic reuse process from the astronaut waste stream which can support a more sustainable waste management strategy for long-duration exploration missions.

Acknowledgments

This work was supported by NASA Space Technology Mission Directorate via collaborative research projects at NASA KSC and NASA MSFC per Center Innovation Fund awards. The authors thank the ISM Team at NASA MSFC, notably Dr. Jennifer Jones and Cadre Francis, for their support of this work. The authors also thank collaborators at the University of Louisville, notably Dr. Kunal Kate, Sihan Zhang, and Fatou Ndiaye. The authors also thank Jason Fischer, Charles Gongora-Richardson and other colleagues in the KSC Applied Chemistry Laboratory and KSC Cleaning, Refurbishment, and Chemical Analysis laborary for their support and use of various testing facilities to accomplish this research.

References

[1] Sanders, Gerald, "ISRU Info : Home of the Space Resources Roundtable," Update on NASA ISRU Plans, Priorities, and Activities. Retrieved 26 February 2024. https://isruinfo.com/public/index.php?page=srr_23

[2] Pitts, R., Olson, J. A., Benson, M., Kelley, M., Richardson-Gongora, C. A., and Meier, A. J., "Development of a Predictive Model for In-Situ Resource Utilization of Space Exploration Waste," *ASCEND 2023*, American Institute of Aeronautics and Astronautics. https://doi.org/10.2514/6.2023-4659

[3] Lynch, C., Goodliff, K. E., Stromgren, C., Vega, J., and Ewert, M. K., "Logistics Rates and Assumptions for Future Human Spaceflight Missions Beyond LEO," *ASCEND 2023*, American Institute of Aeronautics and Astronautics. https://doi.org/10.2514/6.2023-4617

[4] Anthony, S. M., and Hintze, P. E., "Trash-to-Gas: Determining the Ideal Technology for Converting Space Trash into Useful Products."

[5] Olson, J. A., Chai, P., Rinderknecht, D., and Meier, A. J., "A Comparison of Propellant Requirements for Crewed Mars Missions Incorporating Different Waste Processing Technologies," *ASCEND 2021*, American Institute of Aeronautics and Astronautics, 2021. https://doi.org/10.2514/6.2021-4080
[6] Olson, J. A., Rinderknecht, D., Essumang, D. E., Kruger, M. J., Golman, C., Norvell, A., and Meier, A., "A Comparison of Potential Trash-to-Gas Waste Processing Systems for Long-Term Crewed Spaceflight."
[7] Pitts, R., Meier, A., Olson, J., Shah, M., Rinderknecht, D., and Toro Medina, J., "Suborbital Testing of the OSCAR Trash-to-Gas System," 2022. Retrieved 26 February 2024. https://hdl.handle.net/2346/89548
[8] Meier, A. J., Rinderknecht, D., Olson, J., Shah, M. G., Medina, J. A. T., Pitts, R. P., Carro, R. V., Gleeson, J. R., Hochstadt, J., Bell, E. A., Forrester, E. A., Kruger, M., and Essumang, D., "Pioneering the Approach to Understand a Trash-to-Gas Experiment in a Microgravity Environment," *Gravitational and Space Research*, Vol. 9, No. 1, 2021, pp. 68–85.
[9] Prater, T., Werkheiser, N., and Ledbetter, F., "An Overview of NASA's In-Space Manufacturing Project."
[10] Hauser, T., Reisch, R. T., Breese, P. P., Nalam, Y., Joshi, K. S., Bela, K., Kamps, T., Volpp, J., and Kaplan, A. F. H., "Oxidation in Wire Arc Additive Manufacturing of Aluminium Alloys," *Additive Manufacturing*, Vol. 41, 2021, p. 101958. https://doi.org/10.1016/j.addma.2021.101958
[11] Razavi-Tousi, S. S., and Szpunar, J. A., "Effect of Ball Size on Steady State of Aluminum Powder and Efficiency of Impacts during Milling," *Powder Technology*, Vol. 284, 2015, pp. 149–158. https://doi.org/10.1016/j.powtec.2015.06.035
[12] Coker, E., "The Oxidation of Aluminum at High Temperature Studied by Thermogravimetric Analysis and Differential Scanning Calorimetry.," SAND2013-8424, 1096501, 476804, October 2013, pp. SAND2013-8424, 1096501, 476804. https://doi.org/10.2172/1096501
[13] Qian, M., and Schaffer, G. B., "12 - Sintering of Aluminium and Its Alloys," *Sintering of Advanced Materials*, edited by Z. Z. Fang, Woodhead Publishing, 2010, pp. 291–323. https://doi.org/10.1533/9781845699949.3.291
[14] Gupta, R. K., Murty, B. S., and Birbilis, N., "An Overview of High-Energy Ball Milled Nanocrystalline Aluminum Alloys," Springer International Publishing, Cham, 2017. https://doi.org/10.1007/978-3-319-57031-0
[15] Majidi, B., Melo, J., Fafard, M., Ziegler, D., and Alamdari, H., "Packing Density of Irregular Shape Particles: DEM Simulations Applied to Anode-Grade Coke Aggregates," *Advanced Powder Technology*, Vol. 26, No. 4, 2015, pp. 1256–1262. https://doi.org/10.1016/j.apt.2015.06.008